P-Rex2 mediation of synaptic plasticity contributes to bone cancer pain

Qiaochu Fu[1] , **Xiaoxia Huang[2], Shengjun Wan[2], Yang Li[2], Xiaohui Li[2], Shanchun Su[2], Xueqin Xu[2], and Yanqiong Wu[2]**

Abstract

Bone cancer pain (BCP) seriously affects the quality of life; however, due to its complex mechanism, the clinical treatment was unsatisfactory. Recent studies have showed several Rac-specific guanine nucleotide exchange factors (GEFs) that affect development and structure of neuronal processes play a vital role in the regulation of chronic pain. P-Rex2 is one of GEFs that regulate spine density, and the present study was performed to examine the effect of P-Rex2 on the development of BCP. Tumor cells implantation induced the mechanical hyperalgesia, which was accompanied by an increase in spinal protein P-Rex2, phosphorylated Rac1 (p-Rac1) and phosphorylated GluR1 (p-GluR1), and number of spines. Intrathecal injection a P-Rex2-targeting RNAi lentivirus relieved BCP and reduced the expression of P-Rex2, p-Rac1, p-GluR1, and number of spines in the BCP mice. Meanwhile, P-Rex2 knockdown reversed BCP-enhanced AMPA receptor (AMPAR)-induced current in dorsal horn neurons. In summary, this study suggested that P-Rex2 regulated GluR1-containing AMPAR trafficking and spine morphology via Rac1/pGluR1 pathway is a fundamental pathogenesis of BCP. Our findings provide a better understanding of the function of P-Rex2 as a possible therapeutic target for relieving BCP.

Keywords

Bone cancer pain, P-Rex2, AMPAR, Synapse remodeling

Introduction

Approximately 70% of patients with advanced stage cancer are estimated to suffer varying degrees of bone cancer pain (BCP).[1] BCP substantially aggravates suppressed emotion, impairs social functioning, and reduces quality of life, leading to increased morbidity and mortality.[2] Despite the availability of bisphosphonates, nonsteroidal anti-inflammatory drugs and analgesics, Over 50% of patients with BCP report limited pain relief and adverse side effects due to lack of deeper insights into molecular mechanisms of BCP.[3]

Mechanisms of BCP are complex, including both inflammation and neuropathic components involving various interactions among tumor cells, bone cells, inflammatory cells, and neurons.[4,5] These complex processes are modified at the level of peripheral tissues and nerves, as well as at higher levels of the nervous system such as the spinal cord and brain.[6–8] Recent work has recognized that synaptic plasticity of excitatory synapses is function as a prime mechanism underlying BCP.[9–11]

α-Amino-3-hydroxy-5-methyl-4-isoxazolepropionic acid receptor (AMPAR) is glutamate-gated ion channels which is implicated in fast excitatory synaptic transmission in the central nervous system.[12] The alterations of properties and postsynaptic abundance of AMPAR—their number, composition, and translocation to synapses play a pivotal role in various forms of synaptic plasticity.[13–15] Several studies have showed that bone cancer triggered AMPAR membrane trafficking at synapses of spinal dorsal horn

[1]Department of Anesthesiology, Beijing Tiantan Hospital, Capital Medical University, Beijing, People Republic of China
[2]Institute of Anesthesiology & Pain (IAP), Department of Anesthesiology, Taihe Hospital, Hubei University of Medicine, Shiyan, Hubei, China

Corresponding Author:
Yanqiong Wu, Department of Anesthesiology, Institute of Anesthesiology &Pain, Taihe Hospital, Hubei University of Medicine, Shiyan, 442000, China.
Email: 370958160@qq.com

neurons and induced BCP.[9,16] However, specific molecular modulation of AMPAR after BCP is unknown.

The modification of spine structure and function plays a role in underlying synaptic and behavioral plasticity.[17] Since the development and structural remodeling of dendrites and spines depends on actin cytoskeletal reorganization, it is possible that AMPAR regulates dendritic growth and spine morphogenesis by modulating the activity of the actin cytoskeleton.[18–20] The Rho family of small GTPases is critically involved in the regulation of the spine actin cytoskeleton, notably Rac1.[21,22] Activation of Rac1 promotes actin polymerization, resulting in the addition and stabilization of dendritic branches as well as the development and maintenance of spines.[23] P-Rex2 is a Rac-specific guanine nucleotide exchange factor (GEF), which expressed remains high in adult brain regions undergoing synaptic remodeling.[24] P-Rex2 is required for spine and synapse development and it has been shown that a decrease in P-Rex2 expression results in reduced spine density.[25] However, the overall link among P-Rex2 and AMPAR in BCP has not been reported.

In the present study, we first implanted carcinoma cells into the femur of mice to establish a model of BCP. In vivo and in vitro experiments were performed to examine the effects of P-Rex2 on the BCP and the relevant mechanisms.

Materials and methods

Animals

Adult male C57BL/6 mice (22 ± 2g) were provided by the Institute of Laboratory Animal Science, Hubei University of Medicine were housed in private cages at room temperature (RT; 20°C) with a 12 h/12 h light/dark cycle and with food and water available ad libitum. The experimental procedures and protocols were approved by the Animal Care and Use Committee of Hubei University of Medicine (Hubei, China) and were in accordance with the guidelines for pain research on laboratory animals.

Cell cultures

Mouse Lewis lung cancer (LLC) cells were cultured in RPMI 1640 medium. The cell culture medium contained fetal bovine serum (10%, FBS, Gibco), penicillin (50 U/mL), and streptomycin (50 μg/mL). The LLC cells were cultured in a sterile cell incubator, and the RPMI 1640 medium was replaced every 3 days.

BCP model

BCP model was established by inoculating LLC cells into the intramedullary space of adult C57BL/6 male according to previous study.[26] Mice were anesthetized with isoflurane (3% induction and 2% maintenance) and placed on an operating table covered with insulation blanket. After shaving and

sterilization, an arthrotomy was applied to expose the right condyles of the distal femur. Then a 30-gauge needle was inserted into the mice' femur, and a 5 μL suspension of tumor cells (5 μL, 1×10^5 cells) or boiled tumor cells was slowly injected into the intramedullary space. The injection site was sealed by bone wax to prevent leakage of tumor cells.

Lentivirus construction and intrathecal injection

Lentiviral vectors with a green fluorescent protein (GFP) were constructed to stably knockdown the expression of P-Rex2. The vectors GV493 (hU6-MCS-CBh-gcGFP) and P-Rex2 gene (GenBank accession number NM_109,294) were recombined by the Genechem Company (Genechem, Shanghai, China) and were named as sh P-Rex2. The same vector frameworks carrying no gene sequence were used as the negative control lentivirus, named shctrl. The viral titer of the lentivirus was 8.0×10^8 TU/ml. The virus was injected intrathecally 3 days before the establishment of BCP model. Intrathecal injection was performed as previously described.[27] A 10-mm-long 30-gauge disposable needle with 5 μL LV was inserted at the midspinal line above the ileac crest. A successfully dural puncture was indicated by a reflexive tail flick.

Behavior alanalysis

The behavioral of the mice was tested followed the blind principle. Mechanical hyperalgesia of the mice was assessed using the paw withdrawal mechanical threshold (PWMT) with von Frey filaments (Stoelting, Wood Dale, IL). Behavioral assays were carried out on the day before cell implantation (baseline) and then on days 3, 5, 7, 10, 14, 17, and 21 days after BCP surgery. The mice were placed individually on metal mesh platforms in the plexiglass compartments (10 cm×10 cm×15 cm) and habituated for 30 min to allow acclimatization to the new environment. During each measurement, von Frey filaments (0.02–2.0 g bending force) were applied vertically to the ipsilateral hind paw of the mice, and the force (g) was increased until the paw was withdrawn or flinched. The 50% PWMT was defined according to the up-down method.

Immunofluorescence analysis

For immunofluorescence, spinal cord sections were pretreated in 1% Triton X-100 in PBS for 30 min; the slices were blocked with 5% normal donkey serum in PBS for 10 min at RT and incubated with primary antibodies overnight at 4°C. The following primary antibodies were used: rabbit anti- P-Rex2 antibody (HPA015234, 1:200; Sigma, Munich, Germany), rat anti-NeuN antibody (ab279297, 1:200; Abcam, Cambridge, United Kingdom), and mouse anti-PSD95 antibody (ab13552, 1:200; Abcam, Cambridge, United Kingdom). After removing primary antibody, the slices were washed with PBS and incubated with fluorescent conjugated
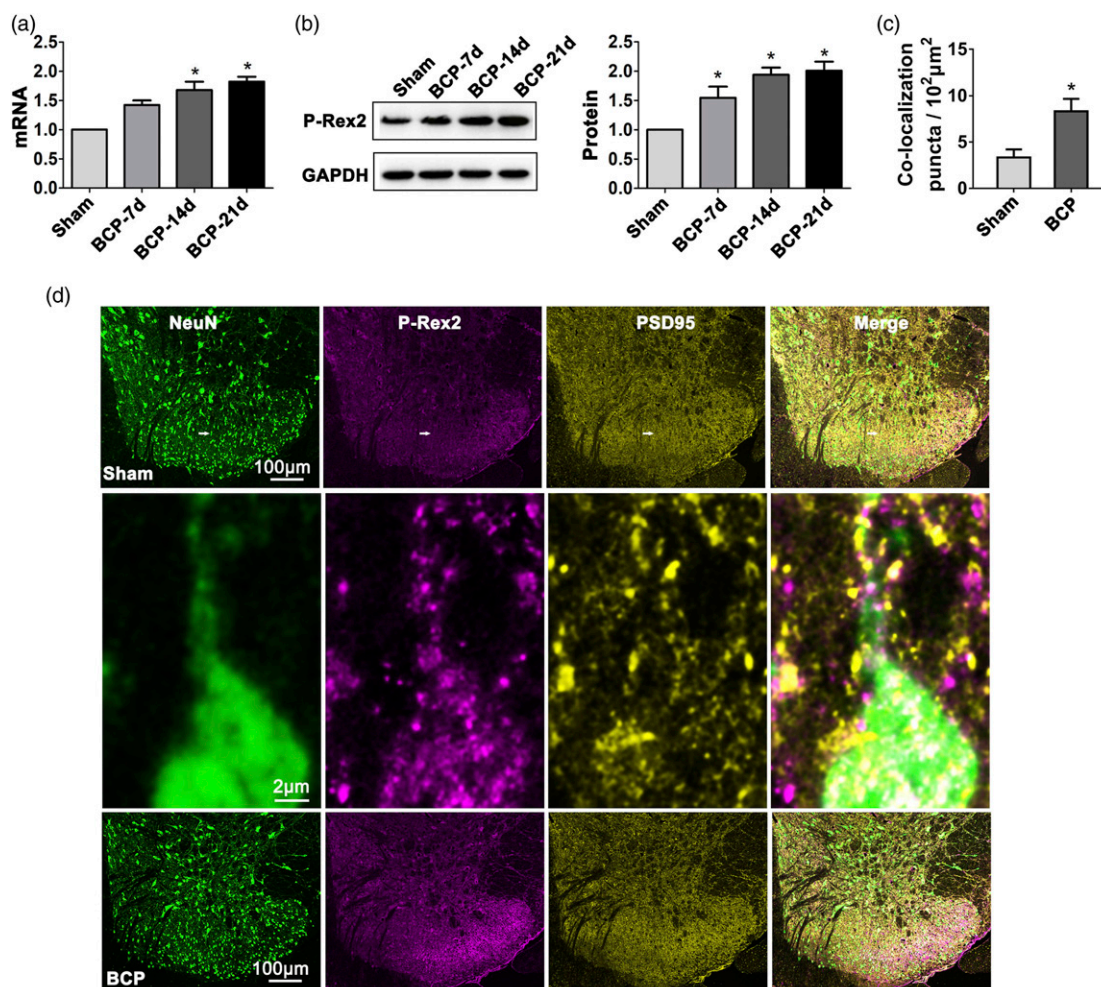
Figure 1. Elevation of P-Rex2 in the spinal dorsal horn initiated by tumor cells implantation. (a) Real-time PCR analysis of P-Rex2 mRNA expression levels in the ipsilateral spinal cord of BCP mice at the indicated time points. Values were expressed as the mean ±SEM, $n = 6$ per group, $*p < .05$ compared with the sham group. (b) Western blotting analysis of P-Rex2 protein expression levels in the ipsilateral spinal cord of BCP mice at the indicated time points. Values were expressed as the mean ± SEM, $n = 6$ per group, $*p < .05$ compared with the sham group. (c) Quantification of P-Rex2, NeuN and PSD95 co-localization puncta. Values were expressed as the mean ± SEM, $n = 6$ per group, $*p < .05$ compared with the sham group. (d) Representative triple staining images of NeuN (green), P-Rex2 (purple), and excitatory postsynaptic marker PSD95 (yellow) in the superficial laminae of the spinal dorsal horn of the mice.

secondary antibodies for 1–1.5 h at 37°C. The sections were examined with a confocal laser microscope (Leica, Germany)

manufacturer. The images were acquired with an Olympus eclipse 80i microscope (Olympus, Japan).

Golgi staining

Mice were deeply anaesthetized with 3% sevoflurane. As described previously,[28] the L4–L6 spinal cord segments were quickly harvested and incubated in the Golgi–Cox solution (FD Neurotechnologies, Rapid Golgi Kit) for 2 weeks at room temperature. The Golgi solution was changed 6 h after the immersion. The fresh brain was then immersed in another Golgi solution for 1 week in the dark. The spinal cord was sectioned at 100 μm thickness in a vibrating microtome and color developed following the instructions from the

Spinal cord slice preparation and patch-clamp recordings

The L4 – L6 spinal cord segments were aseptically removed from the mice under 3.0% sevoflurane anesthesia. The spinal segments were then sliced into transverse slices (350 μm) and incubated at 22–25°C in preoxygenated artificial cerebrospinal fluid solution (ACSF). ACSF contained (in mM): NaCl 126, $MgCl_2$ 2, KCl 3.5, NaH_2PO_4 1.25, $NaHCO_3$ 26, $CaCl_2$ 2, and D-glucose 10. Lamina II in lumbar segments was identified as a translucent band by a television monitor connected to a low light-sensitive charge-
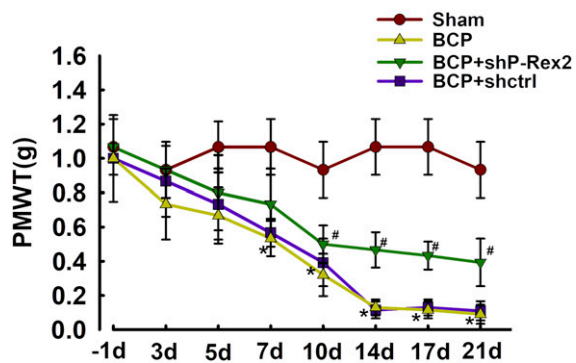
Figure 2. P-Rex2 deficiency attenuated the behavioral hyperalgesia. Changes in PMWT of the ipsilateral paw in the sham, BCP, BCP+shP-Rex2, and BCP+shctrl groups in response to von Frey filaments at the indicated time points. Values were expressed as the mean ±SEM, n = 8 per group. *p < .05 compared with the sham group; #p < .05 compared with the BCP+shctrl group. BCP: bone cancer pain; PMWT: paw withdrawal mechanical threshold.

coupled device camera (710M; DVC, USA).[29] Whole-cell voltage clamp recordings were made from lamina II neurons using patch microelectrodes with the tip openings of 1–2 μm and a series resistance of 3–5 mΩ. The microelectrodes solution contained (in mM): KCl 130, $CaCl_2$ 0.5, HEPES 10, $MgCl_2$ 2, EGTA 10, Mg-ATP 2, and Na-GTP 0.3. The recording data were analyzed using Clampfit 9.0 (Axon Instruments, USA). AMPAR-mediated sEPSC currents were pharmacologically isolated by blocking excitatory N-methyl-daspartate (NMDA) and inhibitory GABAA and glycine receptors with d, l-2-amino-5-phosphonopentanoic acid (AP-5) (50 M), bicuculline (10 M), and strychnine 1 M, respectively. The sIPSC currents were recorded at 0 mV. The recording data were analyzed using Clampfit 9.0 (Axon Instruments, USA).

Quantitative real-time polymerase chain reaction

For the quantitative real-time polymerase chain reaction (q-pcr) analysis, all the mice were deeply anaesthetized with 3% sevoflurane, and the L4–L6 spinal cord was quickly removed and stored at −80°C for analysis P-Rex2 mRNA. Total RNA was extracted from the spinal cord using the Trizol reagent and reverse transcribed following the previous study.[10] The mRNA primer sequences for mouse P-Rex2 were listed as follows: GAPDH: F: 5′-TGTGTCCGTCGTGGATCTGA-3′, R: 5′- CCTGCTTCACCACCTTCTTGA-3′; P-Rex2: F: 5′-GCTGCTTGGAGGTCGGAAGAATAC-3′, R: 5′-CCAT-CACTGCTGTGTAGTCACTATGTC-3′. The expression of the targeted mRNA was analyzed using the formula 2-(Ct target gene - Ct reference gene).

Western blot analysis

After being deeply anaesthetized, the L4–L6 spinal cord was removed and transferred quickly to ice-chilled radio-immunoprecipitation assay (RIPA) lysis buffer. The homogenates were centrifuged at 10,000× g for 15 min at 4°C to separate the total protein from the precipitate. A membrane compartment protein extraction kit (BioChain Institute, Inc., USA) was used to extract the membrane fraction of the dorsal horn. The concentration of the total protein was measured by the BCA protein assay kit. The following primary antibodies were used: rabbit anti- P-Rex2 antibody (1:1000; Sigma), rabbit anti-Rac1 antibody (1:1000, Abcam), rabbit anti-phospho Rac1 plus Cdc42 (1:200, Santa Cruz, USA), rabbit anti- GluR1 antibody (1:1000, Abcam), and rabbit anti-pGluR1 antibody (1:1000, Abcam). Western blot assay was performed as previously described.[11]

Statistical data analysis

All data were analyzed using SPSS 22.0 software, and results are expressed as means ±standard error of the mean (SEM). For the behavioral data, 2-tailed Student's t test (2 groups), one-way ANOVA, or two-way ANOVA followed by post hoc Bonferroni's test. For the other data, comparisons between two groups were performed using two-tailed unpaired Student t-tests; comparisons among various groups were performed using one-way analysis of variance with Tukey post hoc test. The p < .05 was considered statistically significant.

Results

1. Elevation of P-Rex2 in the spinal dorsal horn initiated by tumor cells implantation

To detect whether P-Rex2 increased in the development of BCP, we first examined the expression of P-Rex2 in the lumbar (L4 – L6) spinal dorsal horn. The result of q-pcr and western blot showed that P-Rex2 mRNA and protein of BCP mice increased significantly in a time-dependent manner, starting from day 7 after modeling and maintained for day 21, whereas the levels remained low in sham mice (p < 0.05) (Figures 1(a) and (b)).

We then identify the cellular localization of activated P-Rex2 in the spinal cord. Triple-label immunofluorescence staining of P-Rex2 was performed with neurons neuronal nuclei (NeuN) and PSD95 (an excitatory postsynaptic marker), suggesting that when compared with sham group, the upregulation of P-Rex2 of BCP mice mainly occurs in dorsal horn neurons and was colocalized with PSD95 (p < .05) (Figures 1(c) and (d)). Our data showed that P-Rex2 upregulated in spinal dorsal horn in BCP mice, which might play a role in synaptic regulation.

2. P-Rex2 deficiency attenuated the behavioral hyperalgesia

To further investigate the role of P-Rex2 in BCP, recombinant RNAi lentivirus-targeting P-Rex2 (shP-Rex2) or the control lentivirus (shctrl) was intrathecally injected in BCP mice. As shown in Figure 2, compared with the basic PWMT, injection of LLC cells into the mice femur induced mechanical
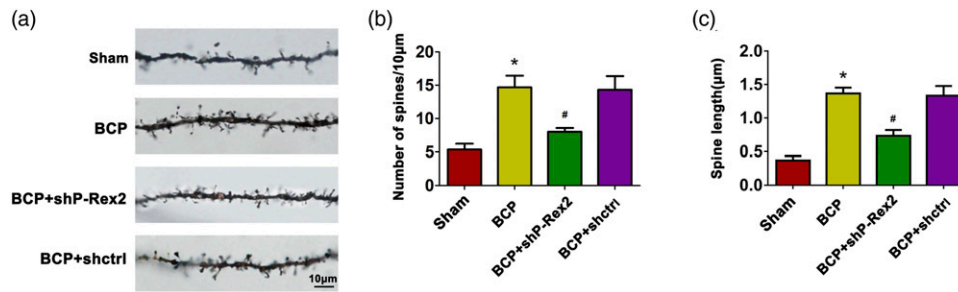
Figure 3. P-Rex2 controls the formation and enlargement of dendritic spine in the spinal dorsal horn of BCP mice. (a) Representative photomicrographs of spine morphology in the dorsal horn in the sham, BCP, BCP+shP-Rex2, BCP+shctrl groups 14-day postsurgery. The spine density (b) and length (c) were assessed. The results were expressed as the mean ±SEM, $n = 6$ per group. $*p < .05$ compared with the sham group; $\#p < .05$ compared with the BCP+shctrl group.
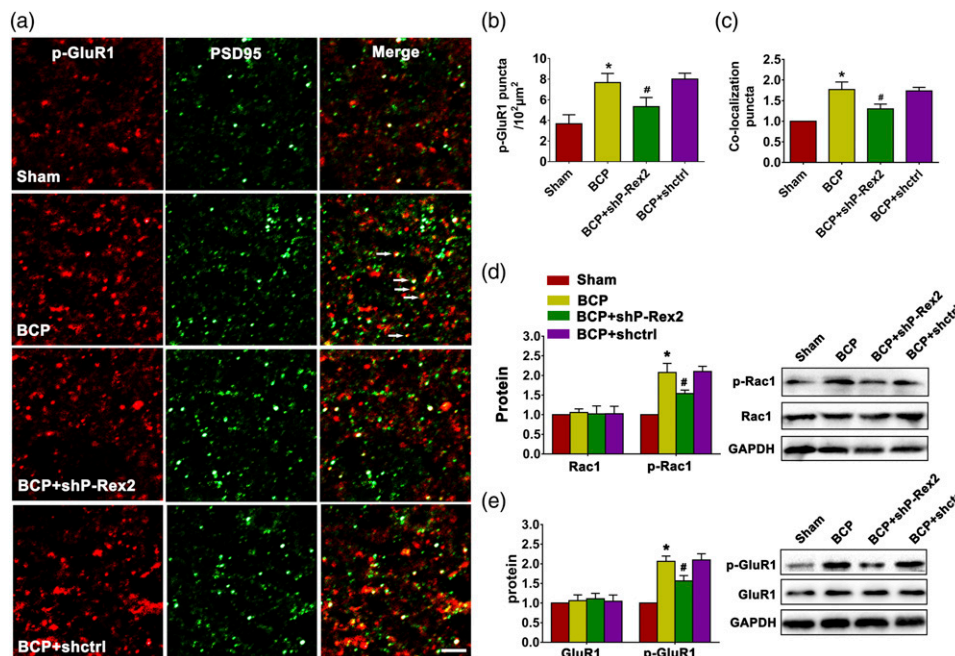

Figure 4. P-Rex2 promoted the phosphorylation level of spinal AMPAR in BCP mice. (a) Double immunostain with p-GluR1 (red) and PSD95 (green) in the superficial laminae of the spinal dorsal horn of the rats. The white arrow points to co-localization puncta. Scale bar: 10 μm. Quantification of p-GluR1 positive puncta (b) and co-localization puncta (c) in the sham, BCP, BCP+shP-Rex2, and BCP+shctrl groups. Values were expressed as the mean ±SEM, $n=6$ per group. $*p < .05$ compared with the sham group; $\#p < .05$ compared with the BCP+shctrl group. (d) Western blot analysis of Rac1 and p Rac1 in the sham, BCP, BCP+shP-Rex2, BCP+shctrl groups 14-day postsurgery. Values were expressed as the mean ±SEM, $n = 6$ per group. $*p < .05$ compared with the sham group; $\#p < .05$ compared with the BCP+shctrl group. (e) Western blot analysis of GluR1 and pGluR1 in the sham, BCP, BCP+shP-Rex2, BCP+shctrl groups 14-day postsurgery. Values were expressed as the mean ±SEM, $n=6$ per group. $*p < .05$ compared with the sham group; $\#p < .05$ compared with the BCP+shctrl group.

hyperalgesia. Treatment with shP-Rex2 but not the shctrl prevented the reduction of PWMT compared with the BCP mice ($p < .05$) (Figure 2). These results suggest that the upregulation of P-Rex2 promoted the development of BCP.

3. P-Rex2 controls the formation and enlargement of dendritic spine in the spinal dorsal horn

Since plasticity of synaptic structure and function plays an essential role in the development of BCP, we then detected whether P-Rex2 could control the formation and enlargement of dendritic spine in the spinal dorsal horn. Golgi staining analysis showed that BCP mice exhibited postoperative spine formation ($p < .05$) and enlargement ($p < .05$) in the dorsal horn when compared with the sham group mice (Figure 3(a), (b) and (c)). As expected, shP-Rex2 reduced spine formation ($p < .05$) and enlargement ($p < .05$) (Figure 3(a), (b) and (c)). Together, these results suggest that P-Rex2 could induce BCP by regulating the remodeling of synaptic structure.
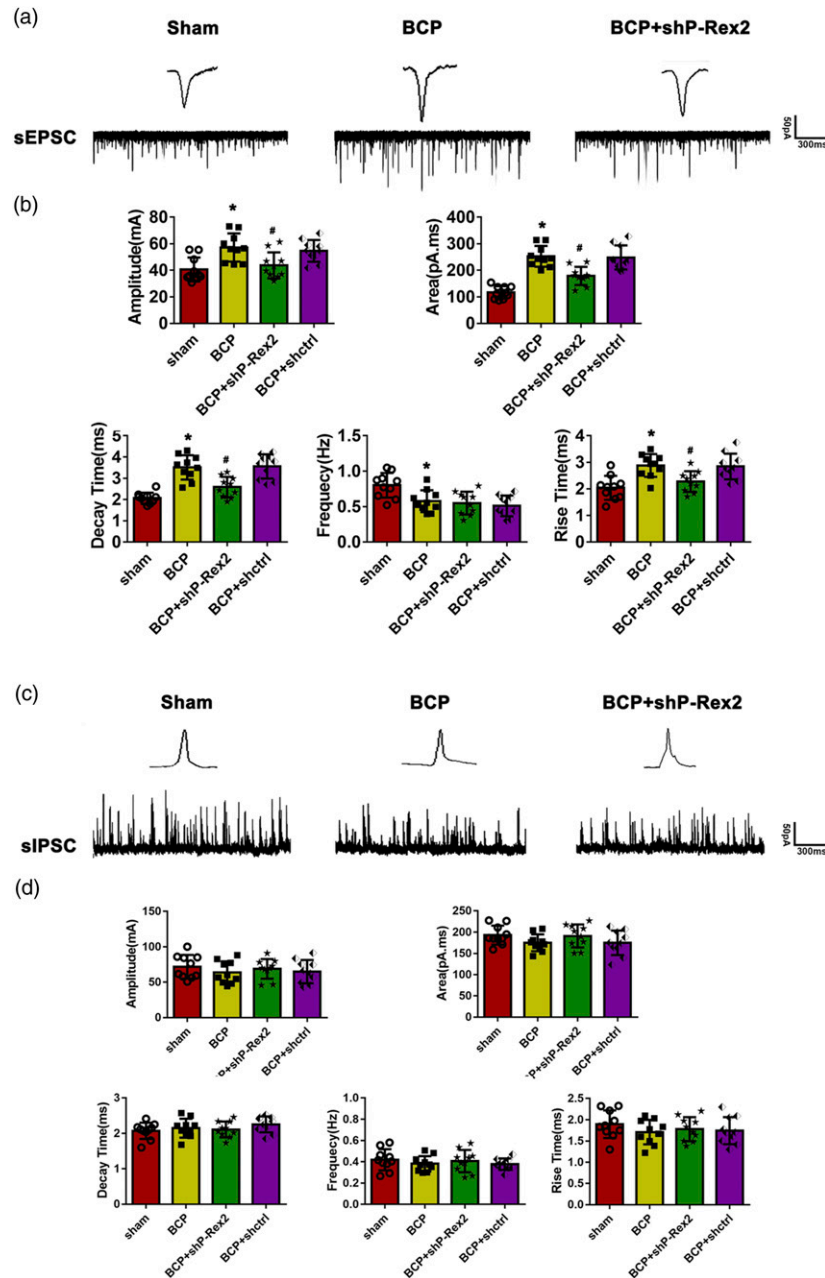
Figure 5. P-Rex2 modulated the electrophysiologic function of spinal AMPA Receptor in BCP. (a) Representative traces of sEPSC in the dorsal horn neurons of spinal cord slices in the sham, BCP, BCP+shPRex2, BCP+shctrl groups 14-day postsurgery. (b) The amplitude, area, rise time, decay time, and frequency of sEPSC in the spinal dorsal horn neurons under different conditions were evaluated. The results were expressed as the mean ± SEM, n = 10 per group. *p < .05 compared with the sham group; #p < .05 compared with the BCP+shctrl group. (c) Representative traces of sIPSC in the dorsal horn neurons of spinal cord slices in the sham, BCP, BCP+shP-Rex2, BCP+shctrl groups 14-day postsurgery. (d) The amplitude, area, rise time, decay time, and frequency of sIPSC in the spinal dorsal horn neurons under different conditions were evaluated. The results were expressed as the mean ± SEM, n = 10 per group.

4. P-Rex2 promoted the phosphorylation level of spinal AMPAR in BCP mice

To study the molecular mechanism of P-Rex2 on the regulation of spinal excitatory synapses we then measured the expression and activity of Rac1 and GluR1 activity in BCP

mice. Our data showed that P-GluR1 was colocalized with PSD95 in the superficial laminae of the dorsal horn (Figure 4(a), (b) and (c)). There was no change in the total protein expression level of Rac1 and GluR1 between the BCP mice and sham group mice (p > .05) (Figures 4(d) and (e)). However, the phosphorylated form of both Rac1 (p-Rac1)

and GluR1 (p-GluR1) was significantly increased in the BCP group than in the sham group ($p < .05$) (Figures 4(d) and (e)). Treatment with shP-Rex2 significantly decreased the expression of p-Rac1 and pGluR1 in the BCP mice, compared with the BCP+shctrl group ($p < .05$), and had no effect on the level of total Rac1 and GluR1. Taken together, these results suggested that P-Rex2 could contribute to the development of BCP by regulating the phosphorylation of AMPAR GluR1 trafficking, which was critical in nociceptive synaptic plasticity.

5. P-Rex2 modulated the electrophysiologic function of spinal AMPAR in BCP

P-Rex2 could increase the expression of AMPAR p-GluR1 in BCP mice; however, its effect on AMPAR electrophysiologic function was still unclear. Thus, the whole-cell patch-clamp recordings were used to find the functional regulation of AMPAR by P-Rex2 in BCP mice. The representative traces of sEPSC in spinal cord dorsal horn neurons after different interventions are shown in Figure 5a. Compared with the sham group, the frequency of AMPAR current was decreased ($p < .05$), whereas the rise time, amplitude, area, and decay time of AMPAR current were increased ($p < .05$) in the BCP group (Figure 5b). Intriguingly, shP-Rex2 application apparently downregulated the increased the rise time, amplitude, area, and decay time of AMPAR current in BCP mice (($p < .05$) (Figure 5b). We then measured the effect of P-Rex2 on sIPSC in spinal cord dorsal horn neurons after different interventions (Figure 5c). Compared with the sham group, the frequency, rise time, amplitude, area, and decay time of IPSC have not changed ($p > .05$) in the BCP group, BCP+shP-Rex2, and BCP+shctrl groups (Figure 5d). Together, these results suggest that P-Rex2 could upregulate the amplitude of the AMPAR mediated sEPSC, that is, synaptic function remodeling and finally contributed to BCP.

Discussion

Cumulative evidence manifests that rapid structural modifications of central excitatory synapses and altered synaptic functional plasticity in neurodevelopmental and psychiatric disorders are tightly correlated.[30–32] The dendritic spine structure is critical for synapse function.[33] P-Rex2, GEF that specifically activates Rac small GTPases, is expressed by neurons in the peripheral and central nervous systems.[25] The present study was applied to determine the role of P-Rex2 in the development of the BCP. Our data have showed that P-Rex2 was upregulated in the spinal dorsal horn of the BCP mice. Compared with mice from the sham group, tumor cells implantation induced BCP from the seventh day. Knockdown of P-Rex2 expression in the dorsal horn by shP-Rex2 alleviated the mechanical hyperalgesia in BCP mice. These results indicated that P-Rex2 participates in the induction and maintenance of BCP.

The immunofluorescence in the spinal cord showed that P-Rex2 was colocalized with NeuN and PSD95 which indicated P-Rex2 mainly expressed in excitatory postsynaptic sites. Since more than 90% of excitatory synaptic transmission occurs at dendritic spines,[34,35] we then detected the change of dendritic spines in the spinal dorsal horn. Interestingly, our data showed that P-Rex2 knockdown decreased the density and the number of dendritic spine in the spinal dorsal horn of BCP mice, which was also consistent with previous study that the decrease of neuronal P-Rex2 leads to abnormalities of neurite outgrowth and finally result in impaired synaptic plasticity.[36] These results suggested that P-Rex2 participated in the regulation of excitatory synapses. It was already well documented that the formation of excitatory synapses could induce spinal central sensitization and contributes to BCP.[10,11] Thus, we thought P-Rex2 might contribute to BCP by regulating excitatory synapse in mice.

P-Rex2 is best known for its roles in cancer, although a vital role in nervous system is emerging.[37,38] P-Rex2 can regulate actin cytoskeleton remodeling by activating Rac GTPases. In the nervous system, Rac1 activity is essential for neurite outgrowth, dendrite branching, and axon pathfinding.[39] Rac1 can increase available anchoring sites in the actin cytoskeleton and induce the clustering of AMPAR in spines.[40,41] Several lines of evidence have showed that the surface trafficking of GluR1 AMPAR from cytosol to postsynaptic membrane lead to nociceptive synaptic plasticity and central sensitization.[42] GluR1 is mainly expressed in superficial layer of spinal dorsal horn and funtion as an initial part of the signal related to the transmission and regulation of pain.[43] In this study, our result showed that the phosphorylated form of both Rac1 (p-Rac1) and GluR1 (p-GluR1) was significantly increased in the BCP group than in the sham group. Treatment with shP-Rex2 significantly inhibited the upregulation of p-Rac1 and pGluR1 in the BCP group. These results suggested that spinal P-Rex2/Rac1/GluR1 activation promoted BCP development. GluR1 AMPAR is highly permeable to Ca^{2+}, which can induce the Ca^{2+} influx and participate in the regulation of synapses transmission and neuronal excitability.[44] Our data showed that, compared with the sham group, the rise time, amplitude, area, and decay time of AMPAR current was increased in BCP group, whereas frequency of AMPAR current was decreased. We speculate that the whole-cell voltage clamp recordings were detected in vitro, and the loss of peripheral noxious stimulation of the spinal cord slices might lead to a decrease in AMPAR current frequency. However, further studies should be needed to explore the specific mechanism. Intriguingly, shP-Rex2 application apparently downregulated the increased rise time, amplitude, area, and decay time of AMPAR current in BCP mice. These results suggested that spinal P-Rex2 can regulate synaptic plasticity through postsynaptic mechanism and ultimately mediate BCP.

In summary, the expression level of P-Rex2 was markedly increased in the spinal dorsal horn of BCP mice. Knockdown

of P-Rex2 expression in the spinal dorsal horn could attenuate the mechanical hyperalgesia in the BCP mice. P-Rex2 mediated excitatory synaptic transmission by regulating Rac1/pGluR1 pathway and reducing the clustering and trafficking of pGluR1 to postsynaptic membranes. These findings suggest that P-Rex2 might be a potential therapeutic target for alleviating BCP.

Authors' contributions

Qiaochu Fu and Yanqiong Wu conceived the project and designed the experiments. Qiaochu Fu and Xiaoxia Huang performed the experiments. Wencui Li, Shengjun Wan, Yang Li, Xiaohui Li, Shanchun Su, and Xueqin Xu analyzed the data. Qiaochu Fu wrote the paper under the guidance of Yanqiong Wu.

Declaration of conflicting interests

The author(s) declared no potential conflicts of interest with respect to the research, authorship, and/or publication of this article.

Funding

ORCID iD

Qiaochu Fu https://orcid.org/0000-0002-3001-0061

References

1. Zajączkowska R., Kocot-Kępska M, Leppert W, Wordliczek J. Bone pain in cancer patients: mechanisms and current treatment. *Int J Mol Sci* 2019; 20: 6047. DOI: 10.3390/ijms20236047.

2. Sindhi V and Erdek M. Interventional treatments for metastatic bone cancer pain. *Pain Manag* 2019; 9: 307–315. DOI: 10.2217/pmt-2018-0073.

3. Glithero C. The challenges of managing bone pain in cancer. *Ulster Med J* 2020; 89: 7–10.

4. Liu S, Lv Y, Wan XX, Song ZJ, Liu YP, Miao S, Wang GL, Liu GJ. Hedgehog signaling contributes to bone cancer pain by regulating sensory neuron excitability in rats. *Mol Pain* 2018; 14: 174480691876756. DOI: 10.1177/1744806918767560.

5. Liu S, Liu YP, Lv Y, Yao JL, Yue DM, Zhang MY, Qi DY and Liu GJ. IL-18 contributes to bone cancer pain by regulating glia cells and neuron interaction. *J Pain* 2018; 19: 186–195. DOI: 10.1016/j.jpain.2017.10.003.

6. Zhang J, Wang L, Wang H, Su Z and Pang X. Neuro-inflammation and central PI3K/Akt/mTOR signal pathway contribute to bone cancer pain. *Mol Pain* 2019; 15: 174480691983024. DOI: 10.1177/1744806919830240.

7. Dai J, Ding Z, Zhang J, Xu W, Guo Q, Zou W, Xiong Y, Weng Y, Yang Y, Chen S, Zhang JM and Song Z. Minocycline relieves depressive-like behaviors in rats with bone cancer pain by inhibiting microglia activation in hippocampus. *Anesth Analg* 2019; 129: 1733–1741. DOI: 10.1213/ANE.0000000000004063.

8. Hu XM, Yang W, Du LX, Cui WQ, Mi WL, Mao-Ying QL, Chu YX and Wang YQ. Vascular endothelial growth factor a signaling promotes spinal central sensitization and pain-related behaviors in female rats with bone cancer. *Anesthesiology* 2019; 131: 1125–1147. DOI: 10.1097/ALN.0000000000002916.

9. Wang H, Li X, Xie X, Zhao H, Gao Y, Li Y, Xu X, Zhang X, Ke C and Liu J. Promotion of bone cancer pain development by decorin is accompanied by modification of excitatory synaptic molecules in the spinal cord. *Mol Pain* 2019; 15: 174480691986425. DOI: 10.1177/1744806919864253.

10. Ke C, Gao F, Tian X, Li C, Shi D, He W and Tian Y. Slit2/robo1 mediation of synaptic plasticity contributes to bone cancer pain. *Mol Neurobiology* 2017; 54: 295–307. DOI: 10.1007/s12035-015-9564-9.

11. Ke C, Li C, Huang X, Cao F, Shi D, He W, Bu H, Gao F, Cai T, Hinton AO Jr. and Tian Y. Protocadherin20 promotes excitatory synaptogenesis in dorsal horn and contributes to bone cancer pain. *Neuropharmacology* 2013; 75: 181–190. DOI: 10.1016/j.neuropharm.2013.07.010.

12. Khan A, Khan S and Kim YS. Insight into pain modulation: nociceptors sensitization and therapeutic targets. *Curr Drug Targets* 2019; 20: 775–788. DOI: 10.2174/1389450120666190131114244.

13. Diering GH and Huganir RL. The AMPA receptor code of synaptic plasticity. *Neuron* 2018; 100: 314–329. DOI: 10.1016/j.neuron.2018.10.018.

14. Roth RH, Cudmore RH, Tan HL, Hong I, Zhang Y and Huganir RL. Cortical synaptic ampa receptor plasticity during motor learning. *Neuron* 2020; 105: 895–908 e895. DOI: 10.1016/j.neuron.2019.12.005.

15. Qu W, Yuan B, Liu J, Liu Q, Zhang X, Cui R, Yang W and Li B. Emerging role of ampa receptor subunit glua1 in synaptic plasticity: implications for Alzheimer's disease. *Cell Prolif* 2021; 54: e12959. DOI: 10.1111/cpr.12959.

16. Dai WL, Yan B, Jiang N, Wu JJ, Liu XF, Liu JH and Yu BY. Simultaneous inhibition of NMDA and mGlu1/5 receptors bylevo-corydalmine in rat spinal cord attenuates bone cancer pain. *Int J Cancer* 2017; 141: 805–815. DOI: 10.1002/ijc.30780.

17. Chidambaram SB, Rathipriya AG, Bolla SR, Bhat A, Ray B, Mahalakshmi AM, Manivasagam T, Thenmozhi AJ, Essa MM, Guillemin GJ, Chandra R and Sakharkar MK. Dendritic spines: revisiting the physiological role. *Prog Neuropsychopharmacol Biol Psychiatry* 2019; 92: 161–193. DOI: 10.1016/j.pnpbp.2019.01.005.

18. Araki Y, Zeng M, Zhang M and Huganir RL. Rapid dispersion of SynGAP from synaptic spines triggers AMPA receptor insertion and spine enlargement during LTP. *Neuron* 2015; 85: 173–189. DOI: 10.1016/j.neuron.2014.12.023.

19. Matsuzaki M, Ellis-Davies GC, Nemoto T, Miyashita Y, Iino M and Kasai H. Dendritic spine geometry is critical for AMPA receptor expression in hippocampal CA1 pyramidal neurons. *Nat Neuroscience* 2001; 4: 1086–1092. DOI: 10.1038/nn736.

20. Yong AJH, Tan HL, Zhu Q, Bygrave AM, Johnson RC and Huganir RL. Tyrosine phosphorylation of the AMPA receptor subunit GluA2 gates homeostatic synaptic plasticity. *Proc Natl Acad Sci* 2020; 117: 4948–4958. DOI: 10.1073/pnas. 1918436117.

21. Li LZ, Yin N, Li XY, Miao Y, Cheng S, Li F, Zhao GL, Zhong SM, Wang X, Yang XL and Wang Z. Rac1 Modulates Excitatory Synaptic Transmission in Mouse Retinal Ganglion Cells. *Neurosci Bull* 2019; 35: 673–687. DOI: 10.1007/s12264-019-00353-0.

22. Costa JF, Dines M and Lamprecht R. The role of Rac GTPase in dendritic spine morphogenesis and memory. *Front Synaptic Neurosci* 2020; 12: 12. DOI: 10.3389/fnsyn.2020.00012.

23. Pennucci R, Gucciardi I and de Curtis I. Rac1 and Rac3 GTPases differently influence the morphological maturation of dendritic spines in hippocampal neurons. *PloS One* 2019; 14: e0220496. DOI: 10.1371/journal.pone.0220496.

24. Barrows D, He JZ and Parsons R. PREX1 protein function is negatively regulated downstream of receptor tyrosine kinase activation by p21-activated kinases (PAKs). *J Biol Chem* 2016; 291: 20042–20054. DOI: 10.1074/jbc.M116.723882.

25. Sherry DM and Blackburn BA. P-Rex2, a Rac-guanine nucleotide exchange factor, is expressed selectively in ribbon synaptic terminals of the mouse retina. *BMC Neurosci* 2013; 14: 70. DOI: 10.1186/1471-2202-14-70.

26. Zhang Z, Deng M, Huang J, Wu J, Li Z, Xing M, Wang J and Guo Q, Zou W. Microglial annexin A3 downregulation alleviates bone cancer-induced pain through inhibiting the Hif-1α/vascular endothelial growth factor signaling pathway. *Pain* 2020; 161: 2750–2762. DOI: 10.1097/j.pain.0000000000001962.

27. Pan Z, Shan Q, Gu P, Wang XM, Tai LW, Sun M, Luo X, Sun L and Cheung CW. miRNA-23a/CXCR4 regulates neuropathic pain via directly targeting TXNIP/NLRP3 inflammasome axis. *J Neuroinflammation* 2018; 15: 29. DOI: 10.1186/s12974-018-1073-0.

28. Das G, Reuhl K and Zhou R. The Golgi-Cox method. *Methods Mol Biol* 2013; 1018: 313–321. DOI: 10.1007/978-1-62703-444-9_29.

29. Fujita T and Kumamoto E. Inhibition by endomorphin-1 and endomorphin-2 of excitatory transmission in adult rat substantia gelatinosa neurons. *Neuroscience* 2006; 139: 1095–1105. DOI: 10.1016/j.neuroscience.2006.01.010.

30. Forrest MP and Parnell E, Penzes P. Dendritic structural plasticity and neuropsychiatric disease. *Nat Reviews Neurosci* 2018; 19: 215–234. DOI: 10.1038/nrn.2018.16.

31. Nanou E and Catterall WA. Calcium Channels, Synaptic Plasticity, and Neuropsychiatric Disease. *Neuron* 2018; 98: 466–481. DOI: 10.1016/j.neuron.2018.03.017.

32. Batool S, Raza H, Zaidi J, Riaz S, Hasan S and Syed NI Synapse formation: from cellular and molecular mechanisms to neurodevelopmental and neurodegenerative disorders. *J Neurophysiol* 2019; 121: 1381–1397. DOI: 10.1152/jn.00833.2018.

33. Berry KP and Nedivi E. Spine dynamics: are they all the same? *Neuron* 2017; 96: 43–55. DOI: 10.1016/j.neuron.2017.08.008.

34. González-Burgos I. From synaptic transmission to cognition: an intermediary role for dendritic spines. *Brain Cogn* 2012; 80: 177–183. DOI: 10.1016/j.bandc.2012.03.002.

35. Harris KM and Kater SB. Dendritic spines: cellular specializations imparting both stability and flexibility to synaptic function. *Annu Rev Neurosci* 1994; 17: 341–371. DOI: 10.1146/annurev.ne.17.030194.002013.

36. Miller MB, Yan Y, Eipper BA and Mains RE. Neuronal Rho GEFs in synaptic physiology and behavior. *Neuroscientist* 2013; 19: 255–273. DOI: 10.1177/1073858413475486.

37. Srijakotre N, Man J, Ooms LM, Lucato CM, Ellisdon AM and Mitchell CA. P-Rex1 and P-Rex2 RacGEFs and cancer. *Biochem Soc Trans* 2017; 45: 963–977. DOI: 10.1042/BST20160269.

38. Donald S, Humby T, Fyfe I, Segonds-Pichon A, Walker SA, Andrews SR, Coadwell WJ, Emson P, Wilkinson LS and Welch HC. P-Rex2 regulates Purkinje cell dendrite morphology and motor coordination. *Proc Natl Acad Sci* 2008; 105: 4483–4488. DOI: 10.1073/pnas.0712324105.

39. Woo S and Gomez TM. Rac1 and RhoA promote neurite outgrowth through formation and stabilization of growth cone point contacts. *J Neurosci* 2006; 26: 1418–1428. DOI: 10.1523/JNEUROSCI.4209-05.2006.

40. Wiens KM, Lin H and Liao D. Rac1 induces the clustering of AMPA receptors during spinogenesis. *J Neurosci* 2005; 25: 10627–10636. DOI: 10.1523/JNEUROSCI.1947-05.2005.

41. Haditsch U, Leone DP, Farinelli M, Chrostek-Grashoff A, Brakebusch C, Mansuy IM, McConnell SK and Palmer TD. A central role for the small GTPase Rac1 in hippocampal plasticity and spatial learning and memory. *Mol Cel Neurosci* 2009; 41: 409–419. DOI: 10.1016/j.mcn.2009.04.005.

42. Peng HY, Chen GD, Hsieh MC, Lai CY, Huang YP and Lin TB. Spinal SGK1/GRASP-1/Rab4 is involved in complete Freund's adjuvant-induced inflammatory pain via regulating dorsal horn GluR1-containing AMPA receptor trafficking in rats. *Pain* 2012; 153: 2380–2392. DOI: 10.1016/j.pain.2012.08.004.

43. Zhu YB, Jia GL, Wang JW, Ye XY, Lu JH, Chen JL, Zhang MB, Xie CS, Shen YJ, Tao YX, Li J and Cao H. Activation of CaMKII and GluR1 by the PSD-95-GluN2B coupling-dependent phosphorylation of GluN2B in the spinal cord in a rat model of type-2 diabetic neuropathic pain. *J Neuropathol Exp Neurol* 2020; 79: 800–808. DOI: 10.1093/jnen/nlaa035.

44. Xie X, Ma L, Xi K, Zhang W and Fan D. MicroRNA-183 Suppresses Neuropathic Pain and Expression of AMPA Receptors by Targeting mTOR/VEGF Signaling Pathway. *Cell Physiol Biochem* 2017; 41: 181–192. DOI: 10.1159/000455987.